The Effect of Modified Blalock-Taussig Shunt Size and Coarctation Severity on Coronary Perfusion After the Norwood Operation

Chiara Corsini, PhD, Giovanni Biglino, PhD, Silvia Schievano, PhD, Tain-Yen Hsia, MD, Francesco Migliavacca, PhD, Giancarlo Pennati, PhD, and Andrew M. Taylor, MD, for the MOCHA Collaborative Group

Laboratory of Biological Structure Mechanics, Politecnico di Milano, Milan, Italy, and Centre for Cardiovascular Imaging, UCL Institute of Cardiovascular Science, and Great Ormond Street Hospital for Children, NHS Foundation Trust, London, United Kingdom

Background. **The size of the modified Blalock-Taussig shunt and the additional presence of aortic coarctation can affect the hemodynamics of the Norwood physiology. Multiscale modeling was used to gather insight into the effects of these variables, in particular on coronary perfusion.**

Methods. **A model was reconstructed from cardiac magnetic resonance imaging data of a representative patient, and then simplified with computer-aided design software. Changes were systematically imposed to the semi-idealized three-dimensional model, resulting in a family of nine models (3-, 3.5-, and 4-mm shunt diameter; 0%, 60%, and 90% coarctation severity). Each model was coupled to a lumped parameter network representing the remainder of the circulation to run multiscale simulations. Simulations were repeated including the effect of preserved cerebral perfusion.**

Results. **The concomitant presence of a large shunt and tight coarctation was detrimental in terms of coronary perfusion (13.4% maximal reduction, 1.07 versus 0.927 mL/s) and oxygen delivery (29% maximum reduction, 422 versus 300 mL $\cdot$ min^{-1} $\cdot$ m^{-2}). A variation in the ratio of pulmonary to systemic blood flow from 0.9 to 1.6 also indicated a "stealing" phenomenon to the detriment of the coronary circulation. A difference could be further appreciated in the computational ventricular pressure–volume loops, with augmented systolic pressures and decreased stroke volumes for tighter coarctation. Accounting for constant cerebral perfusion did not produce substantially different results.**

Conclusions. **Multiscale simulations performed in a parametric fashion revealed a reduction in coronary perfusion in the presence of a large modified Blalock-Taussig shunt and severe coarctation in Norwood patients.**

The Norwood procedure, introduced in 1980 for first-stage palliation of hypoplastic left heart syndrome (HLHS) a few days after birth, involves surgical enlargement of the hypoplastic ascending aorta and placement of a shunt to provide a source of pulmonary blood flow [1]. Given the complex arrangement resulting from the operation, and the intricacy inherent to single-ventricle physiology, observations on the components that can affect this clinical scenario had been made already in the 1980s. One paper, overtly subtitled *The Importance of Coarctation and Shunt Size,* concluded that a more profound understanding of both the pathologic anatomy and the physiology of this condition is essential to obtaining better surgical results [2].

Focusing on the Norwood procedure with a modified Blalock-Taussig (mBT) shunt [3], consensus on optimal shunt size has not been reached. One study observed better hemodynamics with less need for inotropic support early after stage 1 palliation with a larger mBT shunt [4]. Data from another study instead indicated that shunt size does not affect short-term outcomes, with bigger shunt size nevertheless leading to better growth of branch pulmonary arteries [5], although it is also known that effective overshunting can occur with larger shunts and this can be associated with significant morbidity and mortality [6].

An additional complication in this context can be represented by the presence of aortic coarctation. Coarctation in the preductal position in HLHS has been suggested to be caused by the extension of ductal tissue [7]. Recurrent coarctation after stage 1 palliation has been indicated as deleterious, and such recurrent aortic arch obstruction has been associated with compromised right ventricular systolic function at the second stage of palliation [8].

Understanding the effect of mBT shunt size and coarctation severity is therefore of great importance within the context of HLHS surgical palliation, and one

Accepted for publication April 8, 2014.

Address correspondence to Dr Biglino, Centre for Cardiovascular Imaging, UCL Institute of Cardiovascular Science, and Great Ormond Street Hospital, Great Ormond St, London WC1N 3JH; e-mail: g.biglino@ucl.ac.uk.

approach to gather further insight into these variables is represented by computational modeling. A study using multiscale modeling [9] to investigate optimization of shunt placement indicated that a smaller shunt diameter with distal shunt-to-brachiocephalic anastomosis is optimal for systemic oxygen delivery, whereas a more proximal anastomosis is optimal for coronary oxygen delivery, relating coronary artery flow directly to shunt position [10]. Computational modeling has also been used successfully to study the hybrid Norwood [11], highlighting that "retrograde aortic arch hypoplasia or obstruction can lead to suboptimal cerebral and coronary perfusion" [12].

Computational techniques can provide easy access into quantities that can be difficult to measure in vivo, such as coronary perfusion, and offer a way to tackle systematically the problem of the concomitant presence of aortic coarctation and mBT shunt in palliated HLHS. This study thus aims to take advantage of a multiscale modeling strategy to gather insight into the effects of different shunt sizes and coarctation severity on single-ventricle physiology after the Norwood procedure.

Material and Methods

Anatomic Models

A patient with an mBT shunt undergoing second-stage palliation of HLHS was recruited to the Medical University of South Carolina (Charleston, SC). The study was approved by the local institutional review board. Cardiovascular magnetic resonance imaging was performed at 5 months (body surface area [BSA] = 0.33 m^2) before second-stage surgery. The contrast-enhanced, three-dimensional (3D) cardiovascular magnetic resonance dataset was processed to generate an anatomic 3D model (Mimics, Materialise, Leuven, Belgium; see Schievano and associates [13]; Fig 1). The latter was used as the baseline to create an idealized model for this study by means of computer-aided design software (Rhinoceros 3.0, McNeel, Seattle, WA) to control more carefully the caliper of the shunt and the degree of aortic coarctation. Changes of mBT shunt size (3.0-, 3.5-, and 4.0-mm in-ternal diameter) and coarctation severity (0%, about 60%, and 90% lumen reduction, corresponding to 7-, 4.6-, and 2.3-mm isthmus diameter) were implemented in the simplified geometry, thus generating a family of nine models (Fig 2). The choice of coarctation severity was such that the BSA-adjusted smallest aortic cross-section would be less than 56 mm^2/m^2 in both cases, this value having been shown to relate to a considerable gradient

($\geq$20 mm Hg) across the narrowing [14]. Also, in both cases the coarctation index [15] was less than 0.7, which is a parameter considered indicative for recurrent coarctation, as is a maximal instantaneous pressure gradient of greater than 30 mm Hg [15].

Effectively, the only variations among the different 3D models were exclusively the mBT shunt and the coarctation, ensuring for a controlled environment for the simulations. It is worthwhile noting that the Damus-Kaye-Stansel anastomosis present in this patient was used to account for the coronary circulation in the idealized model.

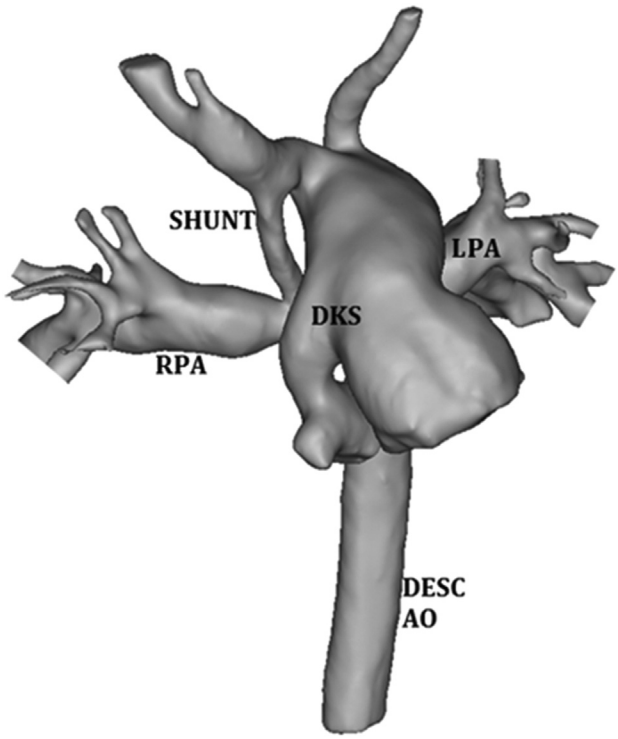

Fig 1. Three-dimensional model of stage 1 anatomy, reconstructed from magnetic resonance imaging data. (DESC AO = descending aorta; DKS = Damus-Kaye-Stansel anastomosis; LPA = left pulmonary artery; RPA = right pulmonary artery; SHUNT = modified Blalock-Taussig shunt.)

The 3D models were discretized using preprocessing software Gambit 2.3.16 (ANSYS Inc, Canonsburg, PA). The mesh density was selected after appropriate sensitivity analysis, ie, progressively doubling the number of elements and ensuring that differences in flow and pressure mean values did not exceed 4%, resulting in approximately 230,000 four-node tetrahedral elements for all 3D models.

Multiscale Modeling

Each 3D model was coupled with a lumped parameter network (LPN). Coupling between the 3D domain and LPN was accomplished by means of interface conditions [9]. The LPN represented the global circulation, comprising five subsystems, ie, heart, upper body and lower body systemic circulations, pulmonary circulation, and coronary circulation [16–18]. The systemic and pulmonary vascular subsystems were, in turn, divided into arterial, capillary, and venous compartments, whose generic description consisted of a linear viscous resistance, constant compliance, and inertance. Time-varying elastances were used to mimic the active and passive behavior of the cardiac chambers, ie, two atria and the single ventricle. Nonlinear resistances simulated the

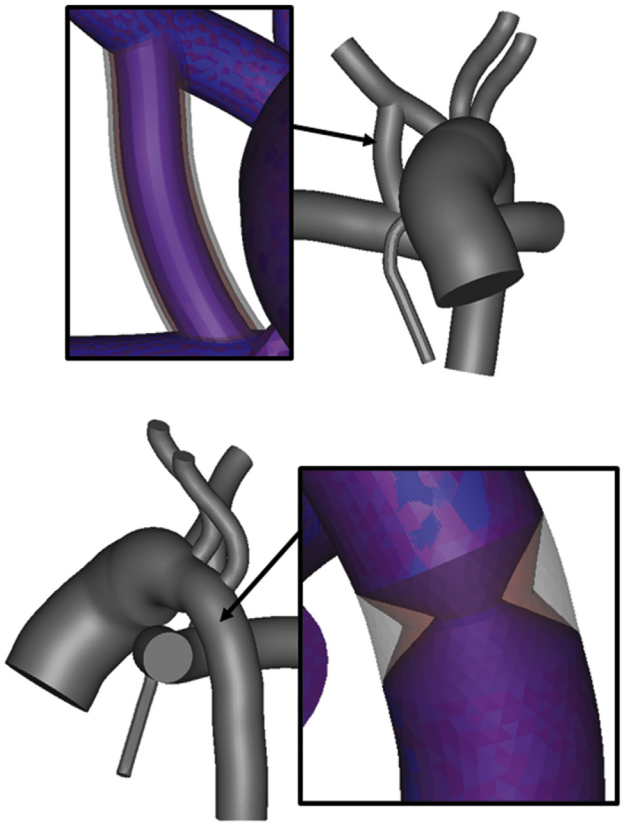

Fig 2. Simplified model of stage 1 anatomy, highlighting variations in modified Blalock-Taussig shunt diameter (top, zoom) and degree of aortic coarctation (bottom, zoom). The arrows indicate the shunt (top) and the region of the aorta where the coarctation is created, past the left subclavian artery (bottom).

valves at the inlet and outlet of the ventricle, whereas a linear resistance replicated the nonobstructive atrial septal defect. Furthermore, a pressure generator in the LPN reproduced the time-varying intramyocardial pressure acting on the coronary circulation. Pulmonary and systemic vascular resistances (PVR and SVR) were set to 3.5 mm Hg $\cdot$ m^2 $\cdot$ min $\cdot$ L^{-1} and 21 mm Hg $\cdot$ m^2 $\cdot$ min $\cdot$ L^{-1}, respectively, with a heart rate of 120 beats/min, reflecting typical stage 1 patient values previously published [19] and also data from patients enrolled in the MOCHA (Modeling of Congenital Hearts Alliance) network (unpublished data), which are reported in Table 1. Blood was assumed to be an incompressible Newtonian fluid with density and dynamic viscosity equal to 1,060 kg/m^3 and 0.005 kg $\cdot$ m^{-1} $\cdot$ s^{-1}, respectively, as previously assumed [16].

Simulations

Pulsatile simulations were run using ANSYS Fluent (ANSYS Inc). The SIMPLE (Semi-Implicit Method for Pressure-Linked Equations) scheme with second-order spatial discretization for momentum and pressure and the first-order implicit transient formulation was chosen

Table 1. Comparison Between the Baseline Model (3.5-mm Modified Blalock-Taussig Shunt, No Aortic Coarctation) and Clinical Values From 5 Patients With Same Characteristics Recruited Within the MOCHA Group (Unpublished Data)

		Clinical Data	
Variable	Model	Mean ± SD	Range
Input			
BSA (m^2)	0.33	0.30 ± 0.04	0.26–0.34
SVR (WU m^2)	21.4	20.1 ± 9.3	13.3–35
PVR (WU m^2)	3.63	2.75 ± 0.81	1.35–3.4
Results			
CO (mL/s)	30.3	27.4 ± 4.1	21–31
$\dot{Q}_{DAo}$ (mL/s)	6.7	4.7 ± 1.2	3–6
$\dot{Q}_P$ (mL/s)	16.5	14.1 ± 4.2	9.7–20
P_{Ao} (mm Hg)	62	56 ± 9	51–72
P_{PA} (mm Hg)	15	13 ± 2	11–16
EDV (mL)	32	31 ± 3	29–35
ESV (mL)	17	14 ± 3	10–18

BSA = body surface area; CO = cardiac output; EDV = end-diastolic volume; ESV = end-systolic volume; MOCHA = Modeling of Congenital Hearts Alliance; P_{Ao} = aortic pressure; PVR = pulmonary vascular resistance; $\dot{Q}_{DAo}$ = descending aortic flow; $\dot{Q}_P$ = pulmonary flow; SVR = systemic vascular resistance.

to solve the Navier-Stokes equations in the 3D domain. The LPN ordinary differential equations were integrated using the explicit Euler time-stepping scheme. Six cardiac cycles were simulated with a time step of 0.1 milliseconds for each multiscale model to reach cyclic repeatability of the solution. Results from the last cycle were used in the analysis. The average execution time was about 2 hours per cycle, using two parallel cluster computer nodes, each with two Quad-Core Intel Xeon E5620 processors.

The first tested model had a 3.5-mm mBT shunt and no aortic coarctation. Results from this simulation, in particular pressure and flow tracings at different locations, were compared with clinical data from 5 Norwood patients from the MOCHA network (unpublished data) to ensure that simulation results were realistic for this patient population. Table 1 summarizes the patients' hemodynamic data as well as the time-averaged values of the modeling results. The BSA, SVR, and PVR were used as input parameters, whereas the other data were used for verification of the model.

After this verification, hemodynamic results were compared for the nine anatomic models. The main outputs of interest in this case were cardiac output, pulmonary flow ($\dot{Q}_P$) and the ratio between pulmonary and systemic blood flow ($\dot{Q}_P/\dot{Q}_S$), cerebral perfusion, and coronary perfusion. Systemic oxygen delivery (SO_2D) and arterial and mixed venous blood oxygen saturations (SatART and SatVEN) were obtained from the oxygen mass balance written for the systemic and pulmonary circulations in stage 1 univentricular arrangement [17]. Briefly, assuming that oxygen consumption (O_2C) in the systemic organs and tissues equals oxygen uptake in the lungs (156.84 mL O_2 $\cdot$ min^{-1} $\cdot$ m^{-2}) and pulmonary vein

saturation equals 98%, SO_2D (mL $O_2 \cdot min^{-1} \cdot m^{-2}$) was calculated as follows:

$$SO_2D = \frac{\dot{Q}_s \cdot C_{art}O_2}{BSA} \quad (1)$$

with $\dot{Q}s$ = systemic flow rate, and $C_{art}O_2$ = oxygen arterial content.

Then, assuming a hemoglobin content (CHb) equal to 16.52 g/dL, and oxygen binding capacity of hemoglobin (HbO_2) of 1.34 mL O_2/g, SatART and SatVEN (%) were calculated as follows:

$$SatART = \frac{SO_2D \cdot BSA}{\dot{Q}_s \cdot CHb \cdot HbO_2} \cdot 100 \quad (2)$$

$$SatVEN = SatART - \frac{O_2C \cdot BSA}{\dot{Q}_s \cdot CHb \cdot HbO_2} \cdot 100 \quad (3)$$

Finally, all simulations were repeated maintaining cerebral blood flow constant with respect to the best-case scenario (ie, 3-mm shunt, no coarctation). This was achieved by adjusting upper body resistance to simulate brain vasodilation. In this case, the value of brain resistance (R_{BR}) was assumed as $R_{BR2} = 0.78 \cdot R_{BR}$. This additional scenario was intended to broadly simulate baroreceptor response, in which brain perfusion is likely to be preserved. All settings and outcomes were the same as those described above.

Results

Comparison between the results from the model with the 3.5-mm mBT shunt and no coarctation with clinical data revealed that the model operated in a range of pressure and flow values in agreement with in vivo values (Table 1). Considering also the variability among different clinical cases, these data confirmed that the model is realistic and representative of Norwood patients, therefore supporting the reliability and relevance of the outcomes of the following simulations. Hemodynamic signals for this model are shown in Figure 3. The realistic nature of the coronary flow signal was verified, both in terms of its mean value and of the shape of the signal—including a small amount of retrograde flow—based on reference values and data from the literature [20, 21].

Results of the nine simulations with all combinations of mBT shunt size and isthmus diameter revealed that the concomitant presence of a large shunt and tight coarctation is detrimental in terms of coronary perfusion (up to 13.4% reduction, 1.07 mL/s versus 0.927 mL/s). All simulation outcomes are summarized in Figure 4. A reduction in cardiac output with increasing coarctation severity was also observed, as well as a reduction in oxygen delivery. A difference could also be appreciated in terms of the shape of the computational ventricular pressure–volume loops (Fig 5), with augmented systolic pressures and decreased stroke volumes for tighter coarctation.

Additional simulations accounting for constant cerebral perfusion did not produce substantially different results, with similar variations in cardiac output, coronary perfusion, and $\dot{Q}_P$ to those observed in the previous case. This is reported in Table 2, which shows the comparison between the best-case scenario (3-mm shunt, no coarctation) and the worst-case scenario (4-mm shunt, 90% coarctation), including simulations of brain vasodilation,

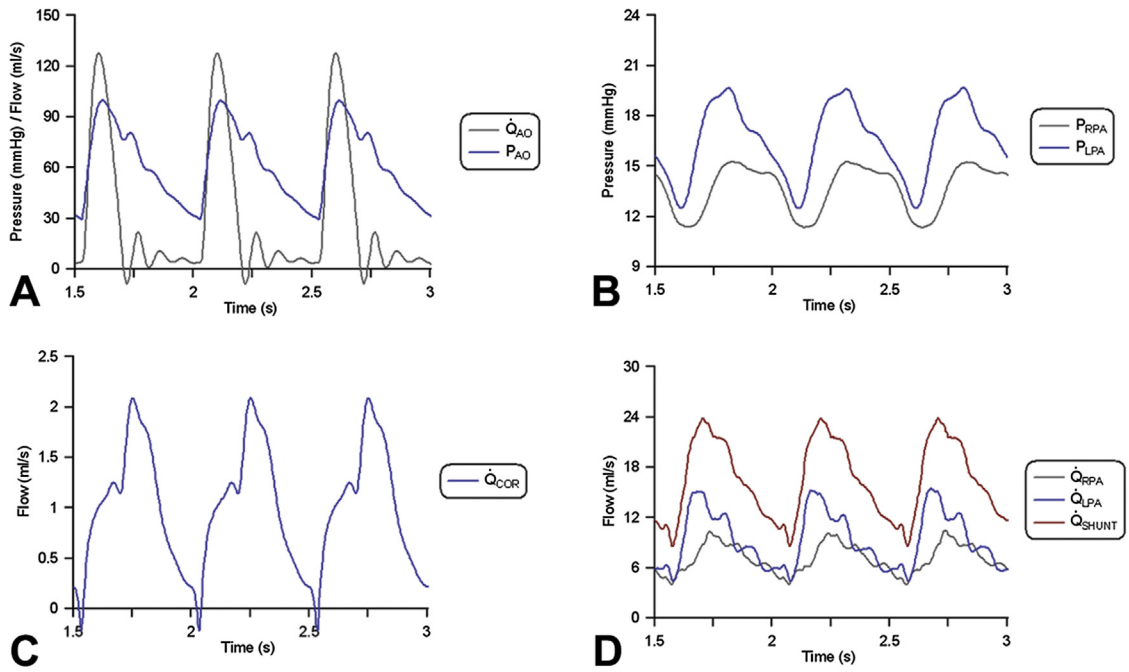

Fig 3. Hemodynamic signals obtained in the baseline model (3.5-mm modified Blalock-Taussig shunt, no aortic coarctation). (A) Aortic flow ($\dot{Q}_{AO}$) and pressure (P_{AO}); (B) right pulmonary artery pressure (P_{RPA}) and left pulmonary artery pressure (P_{LPA}); (C) coronary flow (Q_{COR}); and (D) right pulmonary artery flow (Q_{RPA}), left pulmonary artery flow ($\dot{Q}_{LPA}$), and flow in the modified Blalock-Taussig shunt (Q_{SHUNT}).

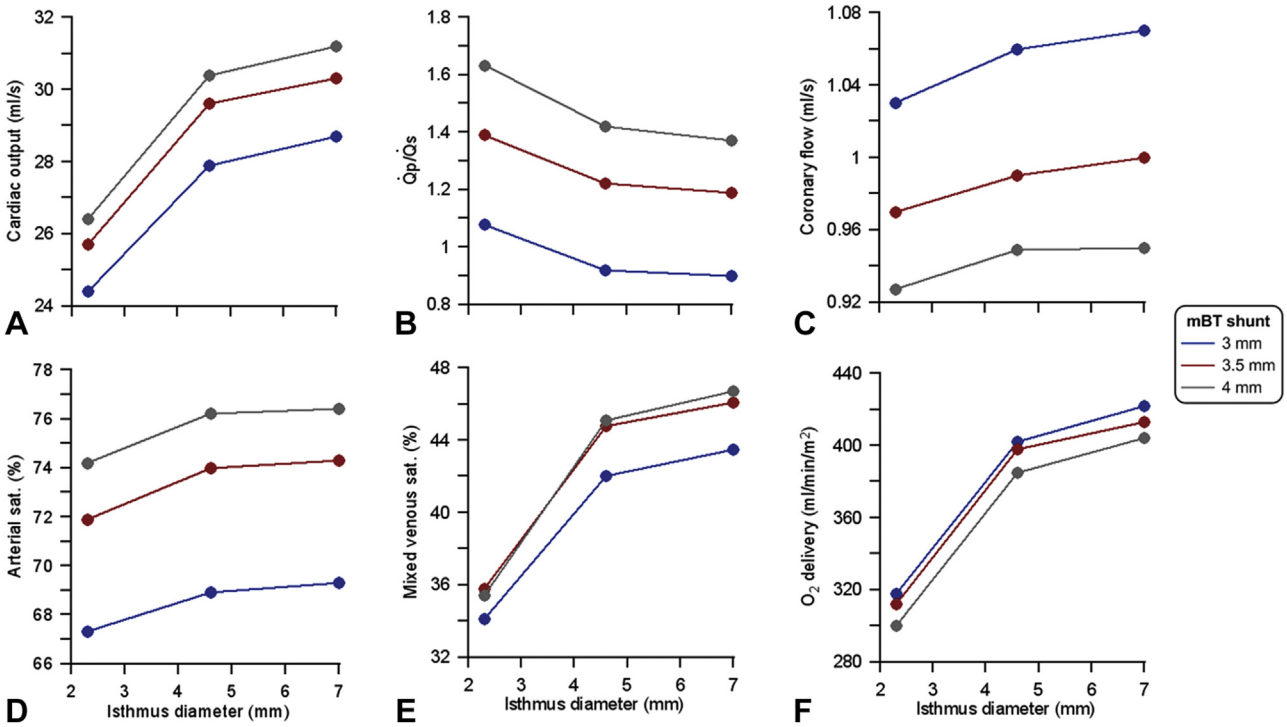

Fig 4. Summary of results for nine models, accounting for all combinations of simulated modified Blalock-Taussig shunt diameters (3.0 [blue], 3.5 [red], and 4.0 [gray] mm) and degrees of coarctation indicated by isthmus diameter. Results indicate changes in (A) cardiac output, (B) ratio of pulmonary to systemic blood flow (Q_P/Q_S), (C) coronary flow, (D) arterial oxygen saturation, (E) mixed venous oxygen saturation, and (F) oxygen delivery.

with the best- and worst-case scenarios defined on the basis of the previous set of simulations. An additional interesting difference between these two extreme cases is a difference in $\dot{Q}_P/\dot{Q}_S$, which increases from 0.9 to 1.5 or 1.6 as the shunt size and the coarctation severity also increase. This indicates the presence of a stealing phenomenon, likely to the detriment of the coronary circulation.

Comment

The physiology between first and second stages of palliation of HLHS is a complex arrangement with a vulnerable balance, affected by several variables ranging from extracorporeal membrane oxygenation [22] to renal complications [23]. Two major geometric variables of great importance for the outcomes of the Norwood procedure are the diameter of the mBT shunt and the presence of aortic coarctation and its severity [2]. Both these parameters can be systematically investigated with a computational approach, which provides a controllable access to data difficult to quantify in this patient population, such as coronary perfusion. A multiscale approach was thus adopted in this study, coupling a family of anatomic models—accounting for a range of mBT shunt

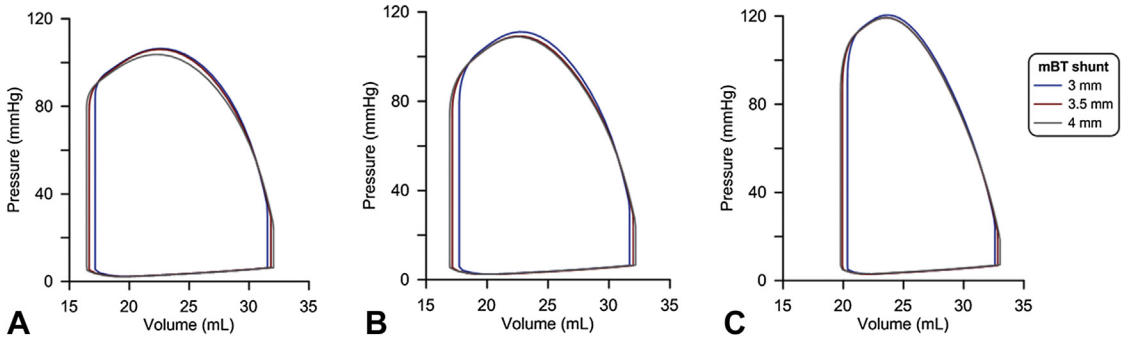

Fig 5. Computational ventricular pressure-volume loops for different combinations of modified Blalock-Taussig shunt sizes (3.0 [blue], 3.5 [red], and 4.0 [gray] mm) and degrees of coarctation. (A) No coarctation (0% lumen reduction); (B) 4.6 mm coarctation (60% lumen reduction); and (C) 2.3 mm coarctation (90% lumen reduction).

Table 2. Comparison Between Best Case Scenario (3.0-mm Modified Blalock-Taussig Shunt, No Aortic Coarctation) and Worst Case Scenario (4.0-mm Modified Blalock-Taussig Shunt, 90% Aortic Lumen Reduction) Among 9 Simulated Combinations of Shunt Size and Coarctation Severity, Including Results for Additional Simulations Assuming That Cerebral Blood Flow Is Preserved

Variable	Best Case	Worst Case	Brain Vasodilation
CoA lumen reduction (%)	…	90	90
Shunt size (mm)	3	4	4
Brain resistance	R_{BR}	R_{BR}	$0.78R_{BR}$
CO (mL/s)	28.7	26.4 (−8%)[a]	26.6 (−7%)[a]
Cerebral flow (mL/s)	3.36	2.69 (−20%)[a]	3.36
Coronary flow (mL/s)	1.07	0.93 (−13%)[a]	0.91 (−15%)[a]
$\dot{Q}_P$ (mL/s)	13.6	16.4 (+21%)[a]	16.1 (+18%)[a]
$\dot{Q}_P/\dot{Q}_S$	0.9	1.6	1.5

[a] Percentages indicate changes from the best-case scenario.

CO = cardiac output; CoA = aortic coarctation; $\dot{Q}_P$ = pulmonary blood flow; $\dot{Q}_S$ = systemic blood flow.

sizes and aortic coarctation dimensions—with an LPN synthesizing the remainder of the single-ventricle circulation.

Having demonstrated that the computational model operates in a realistic range, on the basis of comparison with clinical data, results then focused primarily on variations in coronary perfusion and oxygen delivery. One major finding is represented by the reduction in coronary flow instigated by the concomitant presence of a large mBT shunt (4.0 mm in this case) and narrow aortic coarctation (2.3-mm isthmus diameter). The most likely reason for the observed drop in coronary perfusion is the stealing phenomenon occurring through the large mBT shunt, which clearly can accommodate more pulmonary flow. This observation is supported by a noticeable increase in $\dot{Q}_P/\dot{Q}_S$ (from 0.9 to 1.6), which—clinically—could be falsely reassuring. It should be noted that a similar reduction in coronary flow (approximately 15%) was observed both taking into account preserved cerebral blood flow and not.

The implication of such a reduction in coronary flow is represented by the consequent likely myocardial hypoperfusion. From a physiologic perspective, a reduction in coronary perfusion has been linked with systolic dysfunction in a rat model [24]. This, together with the equally observed reduction in cardiac output, could ensue in a "spiraling effect," ultimately resulting in aggravated ventricular function. In addition, this spiraling phenomenon would be occurring in a physiology that is already compromised, as single-ventricle physiology is, in general, less efficient from the point of view of myocardial oxygen supply–demand balance [25]. And, in this regard, our data report a 29% reduction in oxygen delivery between the best- and worst-case scenarios among the nine simulated anatomies (422 versus 300 mL $\cdot$ min^{-1} $\cdot$ m^{-2}). As there remains significant interstage mortality for HLHS patients [26], such a vicious circle of reduced coronary perfusion, leading to reduced right ventricular function leading to reduced coronary perfusion and so on, might represent the underlying mechanism for the demise of some patients. Hence, these data tell us that although saturation may be high, care must be taken if there is any suggestion of worsening right ventricular function in HLHS patients with large mBT shunts and coarctation.

It should also be remarked that children with HLHS represent a very special group of patients, and with regard to their coronary circulation, it has been suggested that coronary arteries in these patients may also present histologic abnormalities as well as potential mechanisms of accelerated arteriosclerosis [27]. This study did not account for the cellular level, as it was centered on the geometric effects of shunt size and aortic isthmus on the overall hemodynamics.

Finally, this study focused on stage 1 palliation with mBT shunt alone. Other options for sourcing pulmonary blood flow at the time of the Norwood operation include a central shunt from the ascending aorta to the pulmonary arteries [28], a right ventricle-to-pulmonary artery conduit or Sano shunt [29], and the hybrid approach with pulmonary artery banding [11]. In comparing such different options, it has been specifically indicated that one of the advantages of the Sano modification with respect to the Norwood procedure with mBT shunt could lie precisely in the absence of competitive steal of flow from the aortic side and the coronary circulation [30]. Our study not only supports evidence of a competitive steal phenomenon occurring with the mBT shunt but reinforces the concomitant effect of mBT shunt with aortic coarctation, the combination of the two potentially being particularly deleterious.

Limitations

It would be interesting to compare different scenarios in which the patient receives an mBT shunt and may present also with aortic coarctation, eg, HLHS, hypoplastic right heart syndrome, and pulmonary atresia, to generalize these observations even with different underlying ventricular mechanics. This point warrants further investigation in the future, perhaps including data from conductance catheter studies to account for the different scenarios in the multiscale model.

Conclusions

This study took advantage of the capability of multiscale modeling to test, in a parametric fashion, different combinations of mBT shunt diameters and coarctation severity on a realistic model of aortic arch after the Norwood operation. As suggested by early studies in the field [2], results highlighted the importance of these two geometric parameters, and further showed that the simultaneous presence of a large shunt and severe coarctation can have a detrimental effect on coronary perfusion. This, in turn, may account for poor outcome in some Norwood patients.

The authors gratefully acknowledge the support of the following funding bodies: Fondation Leducq, UK National Institute of Health Research, British Heart Foundation, Royal Academy of Engineering/EPSRC, and Heart Research UK. This report is independent research by the National Institute for Health Research Biomedical Research Centre Funding Scheme. The views expressed in this publication are those of the author(s) and not necessarily those of the NHS, the National Institute for Health Research, or the Department of Health.

References

1. Norwood WI, Kirklin JK, Sanders SP. Hypoplastic left heart syndrome: experience with palliative surgery. Am J Cardiol 1980;45:87–91.
2. Jonas RA, Lang P, Hansen D, Hickey P, Castaneda AR. First-stage palliation of hypoplastic left heart syndrome. The importance of coarctation and shunt size. J Thorac Cardiovasc Surg 1986;92:6–13.
3. Yuan SM, Shinfeld A, Raanani E. The Blalock-Taussig shunt. J Card Surg 2009;24:101–8.
4. Photiadis J, Hübler M, Sinzobahamvya N, et al. Does size matter? Larger Blalock-Taussig shunt in the modified Norwood operation correlates with better hemodynamics. Eur J Cardiothorac Surg 2005;28:56–60.
5. Elella RA, Urmatam N, Kalloghian J, Alahmadi M, Alwadaai A. The short and long term effect of Blalock–Taussig shunt size on the outcome after first palliative surgery. J Saudi Heart Assoc 2012;24:278.
6. Dirks V, Prêtre R, Knirsch W, et al. Modified Blalock Taussig shunt: a not-so-simple palliative procedure. Eur J Cardiothorac Surg 2013;44:1096–102.
7. Machii M, Becker AE. Nature of coarctation in hypoplastic left heart syndrome. Ann Thorac Surg 1995;59:1491–4.
8. Larrazabal LA, Selamet Tierney ES, Brown DW, et al. Ventricular function deteriorates with recurrent coarctation in hypoplastic left heart syndrome. Ann Thorac Surg 2008;86:869–74.
9. Quarteroni A, Veneziani A. Analysis of a geometrical multiscale model based on the coupling of PDE and ODE for blood flow simulations. Multiscale Model Simul 2003;1:173–95.
10. Moghadam ME, Migliavacca F, Vignon-Clementel IE, Hsia TY, Marsden AL; Modeling of Congenital Hearts Alliance (MOCHA) Investigators. Optimization of shunt placement for the Norwood surgery using multi-domain modeling. J Biomech Eng 2012;134:051002.
11. Galantowicz M, Cheatham JP, Phillips A, et al. Hybrid approach for hypoplastic left heart syndrome: intermediate results after the learning curve. Ann Thorac Surg 2008;85:2063–71.
12. Baker CE, Corsini C, Cosentino D, et al; Modeling of Congenital Hearts Alliance (MOCHA) Investigators. Effects of pulmonary artery banding and retrograde aortic arch obstruction on the hybrid palliation of hypoplastic left heart syndrome. J Thorac Cardiovasc Surg 2013;146:1341–8.
13. Schievano S, Migliavacca F, Coats L, et al. Percutaneous pulmonary valve implantation based on rapid prototyping of right ventricular outflow tract and pulmonary trunk from MR data. Radiology 2007;242:490–7.
14. Nielsen JC, Powell AJ, Gauvreau K, Marcus EN, Prakash A, Geva T. Magnetic resonance imaging predictors of coarctation severity. Circulation 2005;111:622–8.
15. Lemler MS, Zellers TM, Harris KA, Ramaciotti C. Coarctation index: identification of recurrent coarctation in infants with hypoplastic left heart syndrome after the Norwood procedure. Am J Cardiol 2000;86:697–9.
16. Migliavacca F, Balossino R, Pennati G, et al. Multiscale modelling in biofluidynamics: application to reconstructive paediatric cardiac surgery. J Biomech 2006;39:1010–20.
17. Bove EL, Migliavacca F, de Leval MR, et al. Use of mathematic modeling to compare and predict hemodynamic effects of the modified Blalock-Taussig and right ventricle-pulmonary artery shunts for hypoplastic left heart syndrome. J Thorac Cardiovasc Surg 2008;136:312–20.
18. Hsia TY, Migliavacca F, Pennati G, et al. Management of a stenotic right ventricle-pulmonary artery shunt early after the Norwood procedure. Ann Thorac Surg 2009;88:830–8.
19. Migliavacca F, Pennati G, Dubini G, et al. Modeling of the Norwood circulation: effects of shunt size, vascular resistances, and heart rate. Am J Physiol Heart Circ Physiol 2001;280:H2076–86.
20. Ohye RG, Devaney EJ, Hirsch JC, Bove EL. The modified Blalock–Taussig shunt versus the right ventricle-to-pulmonary artery conduit for the Norwood procedure. Pediatr Cardiol 2007;28:122–5.
21. Donnelly JP, Raffel DM, Shulkin BL, et al. Resting coronary flow and coronary flow reserve in human infants after repair or palliation of congenital heart defects as measured by positron emission tomography. J Thorac Cardiovasc Surg 1998;115:103–10.
22. Tabbutt S, Ghanayem N, Ravishankar C, et al; Pediatric Heart Network Investigators. Risk factors for hospital morbidity and mortality after the Norwood procedure: a report from the Pediatric Heart Network Single Ventricle Reconstruction trial. J Thorac Cardiovasc Surg 2012;144:882–95.
23. Hornik CP, He X, Jacobs JP, et al. Complications after the Norwood operation: an analysis of The Society of Thoracic Surgeons Congenital Heart Surgery Database. Ann Thorac Surg 2011;92:1734–40.
24. Saupe KW, Eberli FR, Ingwall JS, Apstein CS. Hypoperfusion-induced contractile failure does not require changes in cardiac energetics. Am J Physiol 1999;276:H1715–23.
25. Ricci M, Lombardi P, Galindo A, Schultz S, Vasquez A, Rosenkranz E. Effects of single-ventricle physiology with aortopulmonary shunt on regional myocardial blood flow in a piglet model. J Thorac Cardiovasc Surg 2006;132:252–9.
26. Hughes ML, Tsang VT, Kostolny M, et al. Lessons from interstage cardiac magnetic resonance imaging in predicting survival for patients with hypoplastic left heart syndrome. Cardiol Young 2011;21:646–53.
27. Andrews RE, Tulloh RM, Anderson DR, Lucas SB. Acute myocardial infarction as a cause of death in palliated hypoplastic left heart syndrome. Heart 2004;90:e17.
28. Alboliras ET, Chin AJ, Barber G, Helton JG, Pigott JD, Norwood WI. Pulmonary artery configuration after palliative operations for hypoplastic left heart syndrome. J Thorac Cardiovasc Surg 1989;97:878–85.
29. Sano S, Ishino K, Kawada M, et al. Right ventricle-pulmonary artery shunt in first-stage palliation of hypoplastic left heart syndrome. J Thorac Cardiovasc Surg 2003;126:504–10.
30. Rychik J. Hypoplastic left heart syndrome: from in-utero diagnosis to school age. Semin Fetal Neonatal Med 2005;10:553–66.

Appendix

Modeling of Congenital Hearts Alliance (MOCHA) Group: Andrew Taylor, MD, Alessandro Giardini, MD, Sachin Khambadkone, MD, Silvia Schievano, PhD, Marc de Leval, MD, and T.-Y. Hsia, MD (Institute of Cardiovascular Science, University College London, London, UK); Edward Bove, MD, and Adam Dorfman, MD (University of Michigan, Ann Arbor, MI, USA); G. Hamilton Baker, MD, and Anthony Hlavacek, MD (Medical University of South Carolina, Charleston, SC, USA); Francesco Migliavacca, PhD, Giancarlo Pennati, PhD, and Gabriele Dubini, PhD (Politecnico di Milano, Milan, Italy); Alison Marsden, PhD (University of California, San Diego, CA, USA); Jeffrey Feinstein, MD (Stanford University, Stanford, CA, USA); Irene Vignon-Clementel (Inria, Paris, France); Richard Figliola, PhD, and John McGregor, PhD (Clemson University, Clemson, SC, USA).